

# TEMPERATURE COMPENSATED FUSED SILICA RESONATORS USING EMBEDDED NICKEL-REFILLED TRENCHES

*A. Peczalski<sup>1</sup> and M. Rais-Zadeh<sup>1,2</sup>*

<sup>1</sup>Electrical Engineering Department, University of Michigan, Ann Arbor, MI 48109, USA

<sup>2</sup>Mechanical Engineering Department, University of Michigan, Ann Arbor, MI 48109, USA

## ABSTRACT

This paper reports a new fabrication process that utilizes nickel-refilled trenches to achieve passive temperature compensation in fused silica. Using this scheme, piezoelectrically actuated fused silica resonators are demonstrated with a temperature coefficient of frequency (TCF) of +50.28 ppm/K (reduced from +77.65 ppm/K) and quality factors of over 5,000. Additionally, a higher frequency mode at 16 MHz shows a TCF of +21.84 ppm/K (reduced from +71.94 ppm/K). This compensation method can be extended to actuate a compensated and an uncompensated mode of the same device, allowing for a temperature-stable dual-mode frequency reference. This is the first time that passive temperature compensation has been shown for fused silica micro-mechanical resonators.

## KEYWORDS

Fused silica, aluminum nitride, MEMS, resonator, TCF, temperature compensation

## INTRODUCTION

Microelectromechanical resonators have seen a surge of interest over the past twenty years as they strive to replace quartz frequency references with smaller and cheaper micromachined alternatives. While silicon-based resonators have seen commercial success in industrial applications [1], further improvements can be made in the realm of resonator ovenization. By using thermal control to maintain a constant reference frequency, ultra-stable timing references can be created at a fraction of the power, size, and weight of currently available quartz devices.

Fused silica is an appealing material for resonators due to its extremely low internal loss [2, 3] and low thermoelastic damping due to its minimal thermal expansion coefficient. Additionally, the low thermal conductivity of fused silica allows for low-power ovenization while its low thermal expansion coefficient allows for robust single-material packaging. These advantageous material properties make fused silica an excellent choice for ovenized timing references.

Previous investigation of fused silica resonators demonstrated capacitive [4] and piezoelectric resonators [5] with excellent performance, but suffered from extremely large temperature drifts of +90 ppm/K, almost three times that of uncompensated silicon. A fused silica ovenized platform was demonstrated [6], showing a substantial decrease in temperature sensitivity of output frequency but suffered from temperature gradients between the fused silica

frequency reference and the resistive temperature detector, resulting in frequency errors. In order to address both these shortcomings and allow for ultra-stable ovenized fused silica resonators, this paper reports on a passive temperature compensation process for piezoelectric fused silica resonators. Additionally, preliminary results on a dual-mode resonator with varying temperature sensitivity are presented.

## TEMPERATURE COMPENSATED FUSED SILICA RESONATORS

### Temperature Compensation

In order to minimize temperature sensitivity of a resonator it is critical to address its temperature coefficient of frequency (TCF). Similar to passive temperature compensation in silicon, temperature compensation in fused silica can be achieved by utilizing materials with an opposite temperature coefficient of elasticity (TCE) value.

For example, an excellent material choice for passive compensation in silicon is silicon dioxide. Silicon dioxide has a large positive TCE (+180 ppm/K) [5] than can offset the negative TCE (-64 ppm/K) [7] of silicon and is easy to deposit and pattern. The addition of blanket oxide on a silicon resonator can reduce the overall TCF, but has been shown to negatively impact the quality factor ( $Q$ ) [8]. To minimize potential  $Q$  loss, an alternate method of passive temperature compensation has been developed that involves placing compensation material in regions of high stress on the resonator body [9]. Regions of high stress are more sensitive to compensation, allowing for more efficient TCF compensation per unit volume of the compensation material. This compensation method lowers the amount of compensation material required, minimizing  $Q$  degradation and simplifying fabrication issues associated with large amounts of deposited materials.

Fused silica, possessing similar material parameters to deposited silicon dioxide, has a large positive TCE of +180 ppm/K. In order to avoid using a prohibitively large amount of compensation material, it is essential to find a compensation material with a very large negative TCE value, such as some metals. Previously reported efforts to reduce the TCE of glass-blown resonators show that multiple micrometers of blanket-deposited titanium are required for complete compensation [10], which can have a large negative effect on the device performance. In order to minimize the amount of compensation material used, a high negative TCE metal coupled with high-stress region material placement is necessary for such fused silica devices. Nickel is a promising material for this application

due to literature demonstrated TCE values between -1600 ppm/K [11] and -450 ppm/K [12], a low internal loss as compared to other metals [3, 13], and ease of electroplating in large volumes with controllable stress [12].

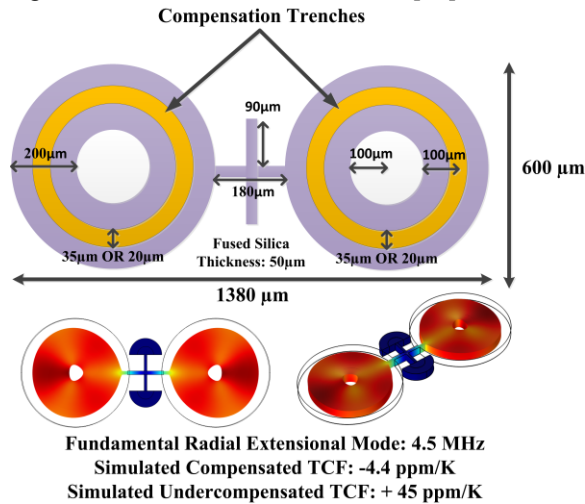


Figure 1: Sketch and simulated mode shapes for a fundamental radial extensional mode of the 50  $\mu\text{m}$  thick dogbone resonator. The nickel trench depth was chosen to be 30  $\mu\text{m}$ , with two chosen trench widths of 35  $\mu\text{m}$  and 20  $\mu\text{m}$ . The simulations assume a nickel TCE of -600 ppm/K.

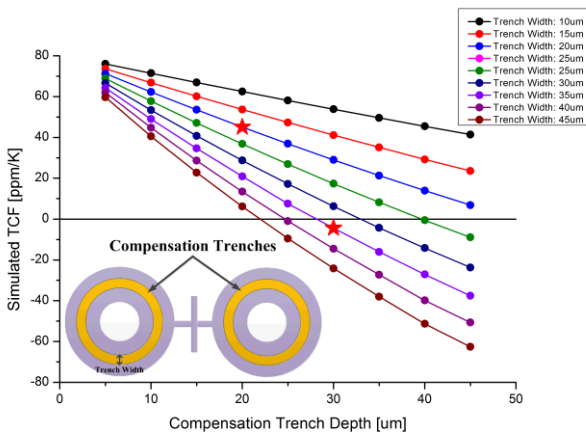


Figure 2: Simulated TCF results for dogbone resonators with varied compensation trench sizes. Starred data points are the selected trench depth/width combinations for the fabricated resonators. Nickel is assumed to have a TCE of -600 ppm/K.

In this work, AlN-on-silica dogbone resonators [5] are temperature compensated through the use of nickel-refilled trenches. Trenches are etched into the resonator body and refilled using nickel electroplating, effectively creating embedded nickel regions in the resonator. Two different widths and depths of the compensation trench were chosen to overcompensate and undercompensate the fundamental radial extensional mode, giving a simulated TCF of -4.4 ppm/K for a 35  $\mu\text{m}$  wide trench and +45 ppm/K for a 20  $\mu\text{m}$

wide trench. These simulations assume a nickel TCE of -600 ppm/K. The dogbone resonator dimensions with a simulated mode shape and TCF is shown in Fig. 1, while the TCF for various nickel-refilled trench dimensions is outlined in Fig. 2. The chosen dimensions were picked to over and undercompensate the fabricated devices to cover a wider range of potential nickel TCE values.

## Device Fabrication

The fabrication process of the passively compensated AlN-on-silica resonators is outlined in Fig 3. The process begins with a 375  $\mu\text{m}$  thick Corning 7980 fused silica wafer. The wafer is etched using a fused silica DRIE process to define the compensation trenches. A 300  $\text{\AA}$  titanium and 5000  $\text{\AA}$  thick gold seed layer is then deposited. The seed layer is sputter deposited to ensure full sidewall coverage of the high aspect ratio compensation trenches. Next, low-stress nickel electroplating is performed to refill the compensation trench. The trench is slightly overplated to ensure total refill and then polished back using mechanical lapping to planarize the surface.

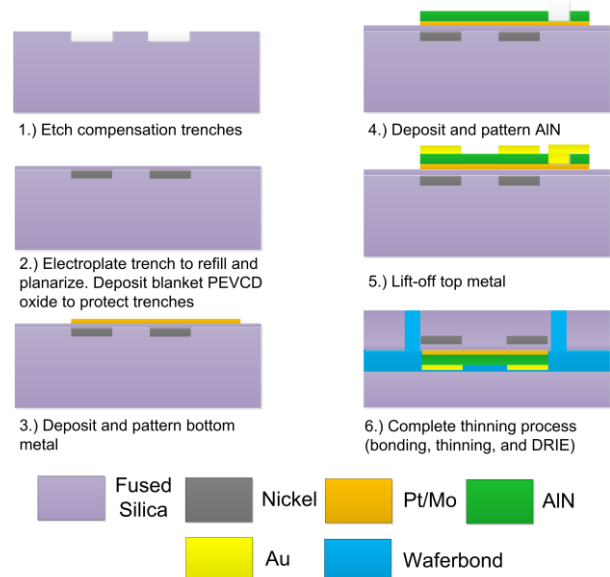


Figure 3: Fabrication flow for compensated fused silica resonators.

After the compensation trenches are planarized, the piezoelectric stack is deposited and patterned. A 100  $\text{\AA}$ /1000  $\text{\AA}$  thick Ti/Pt ground layer is sputtered to ensure high quality AlN growth. Next, 1  $\mu\text{m}$  of AlN is sputtered as the piezoelectric material. Finally, 100  $\text{\AA}$ /1000  $\text{\AA}$  thick Ti/Au layer is deposited to serve as the top metal layer for actuation. The wafer is then flipped and bonded to a fused silica carrier wafer using polymer bonding. The wafer is then thinned using a combination of mechanical lapping a chemical-mechanical polishing (CMP) to a final device thickness of 50  $\mu\text{m}$ . A second fused silica DRIE is performed on the backside of the wafer to define the resonator contour and is then released from the carrier using a solvent. A scanning electron microscope (SEM) image of

the fabricated resonator is presented in Fig. 4, including a cross-section SEM image of a nickel-refilled trench, demonstrating complete trench refill. Due to fabrication non-idealities during the nickel planarization stage, some over-etch of the fused silica surface occurred, decreasing the nickel trench depth to 20  $\mu\text{m}$  from the designed 30  $\mu\text{m}$ . Additionally, a large amount of surface roughness was introduced to the fused silica surface during lapping, negatively affecting the quality of the AlN deposition and reducing the piezoelectric coupling of the device. These issues can be addressed through process adjustments and will be corrected in future fabrication runs.

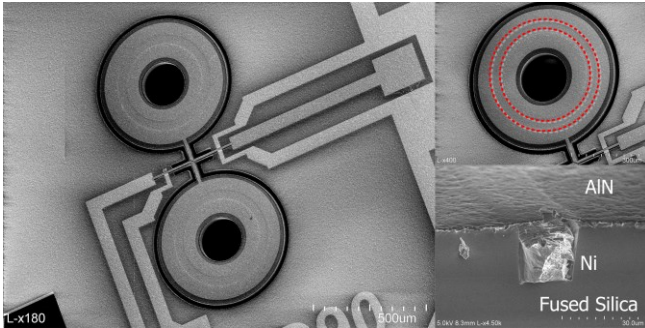


Figure 4: (Left) A SEM image of a fabricated temperature compensated dogbone resonator. (Top right) A zoomed SEM image of a dogbone ring with nickel compensation trench outlined in the center of the ring. (Bottom right) A cross-section SEM image of a nickel-refilled trench with a measured depth of 20  $\mu\text{m}$ .

## MEASURED DEVICE RESULTS

Three types of dogbone resonators are measured and presented in this work. The first design is a fully compensated resonator with the nickel-refilled trench dimensions outlined in Fig. 1. The second design utilizes the undercompensated trench dimensions also seen in Fig. 1. The third design has no nickel-refilled compensation trench and is presented as a reference for performance comparison.

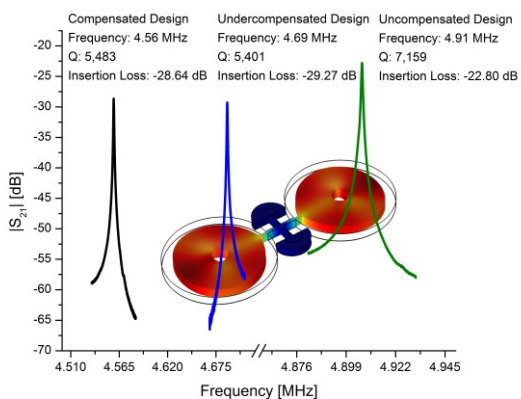


Figure 5:  $S$ -parameter response and measured parameters for a compensated, undercompensated, and uncompensated dogbone in the fundamental radial extensional mode. Background image shows the simulated mode shape.

## Piezoelectric-on-Silica Resonator Response

The  $S$ -parameter responses of the fabricated temperature compensated dogbone resonators were measured using a VNA in a probe station at a pressure less than 10 mTorr. The fundamental radial extensional mode responses for compensated, undercompensated, and uncompensated resonators are presented in Fig. 5.

It can be seen that the measured results of the uncompensated mode do not match the performance seen in earlier generations of the dogbone resonator [5]. While the addition of nickel as a compensation material can reduce the measured  $Q$  of a device, some portion of this difference can be traced back to poor piezoelectric coupling of the AlN film due to deposition on a large surface roughness from the fused silica substrate. Process optimization of the nickel lapping and planarization process will result in a smoother surface and eliminate this coupling issue, significantly improving the performance.

## TCF of Resonators

The TCF of the fabricated resonators were measured using a VNA at a pressure less than 10 mTorr. Measurements at five temperature points were taken between 200 K (-73°C) to 320 K (47°C) and linearly fitted to extract a first-order TCF with a standard fitting error. The measured TCF values for each of the three dogbone designs are shown in Fig. 6.

The measured TCF results show a substantial difference between the simulated fundamental radial extensional mode TCF of -4.4 ppm/K and the measured TCF of +50.3 ppm/K. A portion of this difference between simulation and measured results can be attributed to the smaller-than-designed trench depth for the nickel-refilled trench, but cannot fully explain the difference. This remaining difference can be attributed to the difference between the estimated nickel TCE and the fabricated nickel TCE. By determining the nickel trench dimensions through SEM-based measurements it is possible to fit the TCE of nickel to fabricated device performance. A fitting of the nickel TCE gives a TCE of -100 ppm/K, substantially smaller than the initial estimates reported in literature. Adjusting the device design accordingly will allow for much more accurate TCF compensation for future devices.

Besides the fundamental radial extensional mode, a second, higher frequency mode at 16 MHz was measured that exhibited a substantially different TCF. The TCF for both of these modes are compared alongside their measured  $S$ -parameters in Fig. 7. The 16 MHz mode is significant due to a significant increase in compensation over the fundamental radial extensional mode, from a TCF of +50.3 ppm/K for the fundamental radial extensional mode to a TCF of +21.8 ppm/K for the higher frequency 16 MHz mode. This is a 28.4 ppm/K difference in TCF between the two modes, almost as much as the equivalent TCE of uncompensated silicon. This significant difference in TCF between the two modes allows for applications in dual-mode resonators. By utilizing one highly compensated mode

as a timing reference and the high-TCF mode for temperature sensing, residual temperature gradients on an ovenized device can be eliminated by sharing the same device volume for the timing reference and the temperature sensor.

This demonstration of two separate modes with significantly different TCFs on the same resonator body is an important first step in achieving a highly accurate, small form factor ovenized system. Future work will involve demonstrating a fully compensated resonant mode and further investigation of alternate device modes with different TCF values to achieve dual-mode operation on a single resonator volume.

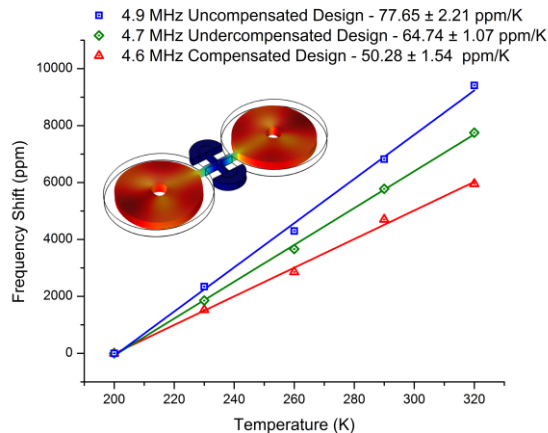


Figure 6: Measured TCF data for the uncompensated dogbone design.

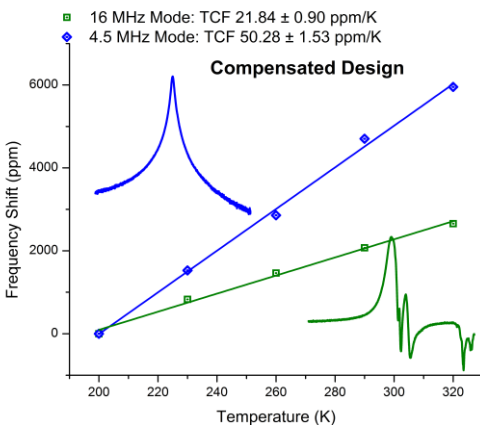


Figure 7: Measured TCF data comparing a compensated fundamental radial extensional mode with a higher frequency mode. A 28.5 ppm/K difference in TCF is seen between the two modes. Insets show the measured S-parameter response for each mode.

## CONCLUSION

This work demonstrates a new fabrication method to passively compensate AlN-on-silica resonators. By utilizing nickel-refilled trenches in regions of high stress, the TCF of a dogbone resonator in the fundamental radial extensional mode is reduced from +77.6 ppm/K to +50.3 ppm/K.

Simultaneously, a second mode on the same device demonstrates a substantially larger TCF shift, decreasing the TCF from +71.9 ppm/K to just +21.8 ppm/K. The difference between the two modes creates a TCF gap of 28.4 ppm, suggesting the possibility of dual-mode operation on the same device volume for use in ovenized frequency reference systems.

## ACKNOWLEDGEMENTS

This work was supported by DARPA under Single-chip Timing and Inertial Measurement Unit (TIMU) program, award #N66001-11-C-4170. The authors would like to acknowledge the OEM group in Gilbert, AZ for assistance in AlN deposition and the staff at the Michigan Lurie Nanofabrication Facility (LNF).

## REFERENCES

- [1] H. Lee *et al*, "Low jitter and temperature stable MEMS oscillators," *Tech. Digest IEEE IFCS*, 2012, pp. 1-5.
- [2] S. D. Penn *et al*, "High quality factor measured in fused silica," *Rev. Sci. Instrum.*, vol. 72, pp. 3670, 2001.
- [3] V. B. Braginsky, V. P. Mitrofanov and V. I. Panov, *Systems with Small Dissipation*. Chicago, IL: The University of Chicago Press, 1985.
- [4] Y. Hwang *et al*, "Fabrication of electrostatically-actuated, in-plane fused quartz resonators using silicon-on-quartz (SOQ) bonding and quartz DRIE," *Proc. IEEE MEMS*, 2009, pp. 729-732.
- [5] Z. Wu *et al*, "Piezoelectrically transduced high-Q silica micro resonators," *Proc. IEEE MEMS* 2013, pp. 122-125.
- [6] Z. Wu *et al*, "Low-power ovenization of fused silica resonators for temperature-stable oscillators" *Tech. Digest IEEE IFCS*, 2014, pp. 1-5.
- [7] M. A. Hopcroft *et al*, "What is the Young's modulus of silicon?" *J. Microelectromech. Syst.*, vol. 19, pp. 229-238, 2010.
- [8] R. Tabrizian *et al*, "A 27 MHz temperature compensated MEMS oscillator with sub-ppm instability," in *Proc. IEEE MEMS*, 2012, pp. 23-26.
- [9] V. A. Thakar *et al*, "Piezoelectrically transduced temperature-compensated flexural-mode silicon resonators," *J. Microelectromech. Syst.*, vol. 22, pp. 815-823, 2013.
- [10] Giner, J. *et al*, "Glass-blown Pyrex resonator with compensating Ti coating for reduction of TCF," *Intl. Symp. ISSS*, 2014, pp. 25-26.
- [11] L. L. Chu *et al*, "Temperature coefficients of material properties for electrodeposited MEMS," *Proc. IEEE MEMS*, 2001, pp. 68-71.
- [12] M. W. Putty, "Micromachined vibrating ring gyroscope," Ph.D. Dissertation, U. of Michigan, 1995.
- [13] W. Huang, *et al*, "Nickel vibrating micromechanical disk resonator with solid dielectric capacitive-transducer gap," *Tech. Digest IEEE IFCS*, 2006, pp. 839-847.

## CONTACT

- \* A. Peczkalski; peczkalsk@umich.edu
- \* M. Rais-Zadeh; minar@umich.edu